Analysis of P-wave Changes for Prediction of Atrial Fibrillation Episodes

Cristina Moreno[1,2], Alba Martín-Yebra[2,1], Aleksei Savelev[3], Pyotr Platonov[4], Pablo Laguna[1,2], Juan Pablo Martinez[1,2]

[1] BSICoS Group, I3A, IIS Aragon, University of Zaragoza, Zaragoza
[2] Centro de Investigación Biomédica en Red – BBN (CIBER-BBN), Zaragoza, Spain
[3] St. Petersburg State University, St. Petersburg, Russia
[4] Department of Cardiology, Lund University Hospital, Lund, Sweden

Abstract

The aim of this study is to assess the value of P-wave morphology markers in sinus rhythm to predict the imminence of atrial fibrillation (AF) episodes in patients with paroxysmal AF (PxAF). P-wave signal-to-noise ratio (SNR) is emphasized by signal processing methods based on principal component (PCA) and periodic component (πCA), together with time averaging analysis. The P-wave morphology features considered are: total power, relative power components, power at high frequency bands (as a measure of rugosity) and P-wave duration. Features are evaluated at three different five-minute time intervals before AF episode occurrences (at 5 minutes, 30 minutes and 60 minutes before the episode onset) in PxAF patients. Results show that in PxAF patients the relative power of the second-to-first principal component increases and the mean duration of the first principal and periodic P-wave component also increases when the time interval gets closer to the AF episode onset. No significant differences were observed in P-wave rugosity by none of both methods. These findings can be interpreted as P wave becoming more complex and wider at the imminence of AF episodes.

1. Introduction

Atrial fibrillation (AF) is the most frequent arrhythmia in clinical practice, increasing the risk of stroke and all-cause mortality. It represents a great socioeconomic burden responsible for approximately one third of hospital admissions by heart rhythm disturbances [1]. The aging of the population has made it one of the most serious health problems in developed countries [2]. AF usually initiates with a paroxysmal activity (PxAF), with the subject having sinus rhythm, with interleaved AF episodes.

In this context, the objective of the study is to evaluate the observations made at some works, [3, 4], who hypothesized that P-wave morphology can be a non-invasive marker of predisposition to AF. In [3], it is hypothesized that the slower conduction in the atria, and the presence of fibrosis in the atrial myocardium, both associated to AF, lead to P-wave widening, with higher complexity and rugosity.

Morphological P-wave parameters such as power, relative power components, power at high frequency bands and duration, computed on the lead transformed P wave were automatically measured during 5 minutes excerpts in patients with PxAF. Values measured at 60, 30 and 5 min before an AF episode where compared with each other.

2. Data

The dataset contains 37 ambulatory ECG recordings from subjects with PxAF, with an average recording duration of 104 hours (range: 21-156 hours). The database was recorded at the state University of St. Petersburg, Russia [5]. Two records were discarded due to poor signal quality and the presence of too many abnormal beats, respectively, resulting in a total of 35 analyzed records.

Thirty-one of the analyzed subjects had 3-lead recordings with a sampling rate of 257 Hz while the remaining four subjects had 12-lead recordings with a sampling rate of 250 Hz.

3. Methods

3.1. ECG Pre-processing

Baseline wander was attenuated at the ECG by using a forward-backward linear 4th-order Butterworth high-pass filter with cutoff frequency of 0.5 Hz [6]. A low-pass filter with the same technique and cutoff frequency of 50 Hz is subsequently used to remove high-frequency muscle noise.

3.2. ECG Segmentation

Preliminary annotation of AF episodes were available from a previous work [5], based on QRS detection with a wavelet-based algorithm [7] followed by AF detection based on fuzzy logic [8]. Thereafter, manual review was performed to finalize the annotation process accomplished by an expert on AF analysis.

The recordings are segmented into 5 minutes duration excerpts, taken at 60, 30 and 5 minutes before the onset of each selected AF episode. All episodes not preceded by an AF-free interval of at least one hour were discarded.

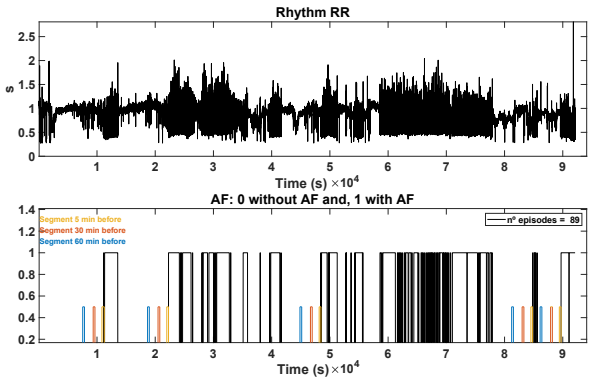

Figure 1. RR interval series in a recording from the dataset (top) and the selected AF episodes with their preceding analyzed excerpts at sinus rhythm (bottom)

3.3. P-wave extraction

Since P waves have typically low signal-to-noise ratio (SNR), we apply linear spatial transformations aiming at improving the SNR by exploiting spatial redundancy in multilead ECG recordings. We used two different processing methods, based on the analysis of principal and periodic components [9].

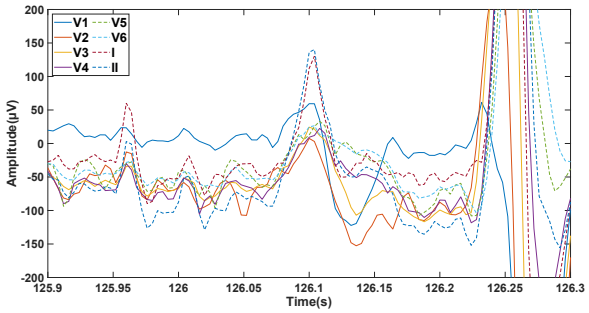

Figure 2. P wave from Recording #1, 60 min before an AF episode

For each analyzed excerpt, beats are extracted and aligned considering the QRS fiducial point as the reference for alignment.

From each *k*-th beat of each *l*-th lead, we segmented a time window of 160 ms, starting 214 ms before the QRS mark, to ensure that it includes the complete P wave. Visual inspection confirmed no overlap between each T wave and its subsequent P wave. Isoelectric level at the P waves was dealt with by offset-correcting each P-wave onset to zero amplitude. The resulting P wave was contained at the column vector $\mathbf{p}_{k,l}$,

$$\mathbf{p}_{k,l} = \begin{bmatrix} p_{k,l}(0) & p_{k,l}(1) & \dots & p_{k,l}(N-1) \end{bmatrix}^T, \quad (1)$$

where N is the number of samples in the P-wave window, $k \in \{1, \dots, K\}$, with K the total number of beats, and $l \in \{1, \dots, L\}$, with L the number of leads. Piling together the k-th P waves from all L leads into a matrix $\mathbf{P}_k$, we have

$$\mathbf{P}_k = \begin{bmatrix} \mathbf{p}_{k,1} & \mathbf{p}_{k,2} & \dots & \mathbf{p}_{k,L} \end{bmatrix}^T, \quad (2)$$

whose n-th column contains the P-wave amplitudes of the L leads at sample n of the k-th beat. Concatenating the K $\mathbf{P}_k$ matrices from subsequent beats a data matrix $\mathbf{P}$ is formed as

$$\mathbf{P} = \begin{bmatrix} \mathbf{P}_0 & \mathbf{P}_1 & \dots & \mathbf{P}_{K-1} \end{bmatrix}, \quad (3)$$

with each l-th row containing samples of the segmented P waves concatenated for the consecutive K beats. Finally a matrix,

$$\mathbf{P}^{(m)} = \begin{bmatrix} \mathbf{P}_m & \mathbf{P}_{m+1} & \dots & \mathbf{P}_{K-1+m} \end{bmatrix}, \quad (4)$$

is built which is similar to $\mathbf{P}$, but with an offset of m beats forward.

3.3.1. PCA followed by beat averaging

This method uses a spatial PCA transformation, where the first principal component is the one maximizing the energy of the signal, followed by the beat averaging, on the first three PCA components. The $L \times L$ matrix $\mathbf{\Psi}_{\text{PCA}}$ defines an orthornomal transformation,

$$\mathbf{Y} = \mathbf{\Psi}_{\text{PCA}}^T \mathbf{P}, \quad (5)$$

whose l-th transformed lead, rows in $\mathbf{Y}$, contains the l-th principal component of data in $\mathbf{P}$. The transformation matrix $\mathbf{\Psi}_{\text{PCA}}$ is obtained by solving the eigenvector problem,

$$\mathbf{R_P} \mathbf{\Psi}_{\text{PCA}} = \mathbf{\Psi}_{\text{PCA}} \mathbf{\Lambda}, \quad (6)$$

where $\mathbf{\Lambda}$ is the eigenvalue diagonal matrix with the eigenvalues sorted in descending order, and $\mathbf{R_P}$ is the spatial correlation of $\mathbf{P}$ estimated as

$$\hat{\mathbf{R}}_P = \frac{1}{KN} \mathbf{P}\mathbf{P}^T \quad (7)$$

3.3.2. πCA followed by beat averaging

With this method, the signal is transformed using the periodic component analysis (πCA), based on the transformation

$$\mathbf{Y} = \mathbf{\Psi}_{\pi\text{CA}}^T \mathbf{P}, \tag{8}$$

that maximizes the m-beat periodic structure of the P wave at the transformed leads in the l-th rows of $\mathbf{Y}$. Afterwards, the average beat of the first three periodic components is computed. The πCA transformation is computed by minimizing

$$\epsilon(\mathbf{w}, m) = \frac{||\mathbf{y}_1^{(m)} - \mathbf{y}_1||^2}{||\mathbf{y}_1||^2}, \tag{9}$$

where $\mathbf{y}_1$ is the first row of $\mathbf{Y}$, $\mathbf{y}_1^{(m)}$ their equivalent when $\mathbf{P}$ is replaced by $\mathbf{P}^{(m)}$ in (8) and $\mathbf{w}$ are the weights in the first row in $\mathbf{\Psi}_{\pi\text{CA}}^T$. Equation (9) can be rearranged as [10]

$$\epsilon(\mathbf{w}, m) = \frac{\mathbf{w}^T \mathbf{R}_{\Delta\mathbf{P}}^{(m)} \mathbf{w}}{\mathbf{w}^T \mathbf{R}_{\mathbf{P}} \mathbf{w}}, \tag{10}$$

where $\mathbf{R}_{\mathbf{P}}$ is defined in (7) and $\mathbf{R}_{\Delta\mathbf{P}}^{(m)}$ is estimated as

$$\hat{\mathbf{R}}_{\Delta\mathbf{P}}^{(m)} = \frac{1}{KN} (\mathbf{P}^{(m)} - \mathbf{P})(\mathbf{P}^{(m)} - \mathbf{P})^T. \tag{11}$$

The weights $\mathbf{w}$ that minimize (10) are given by the generalized eigenvector corresponding to the smallest generalized eigenvalue of the matrix pair $(\mathbf{R}_{\Delta\mathbf{P}}^{(m)}, \mathbf{R}_{\mathbf{P}})$ [10, 11].

The transformation matrix $\mathbf{\Psi}_{\pi\text{CA}}$ is chosen as the generalized eigenvector matrix of the matrix pair with the eigenvectors sorted according to the corresponding eigenvalues in ascending order of magnitude.

3.4. Morphological P-wave features

Each of the previously described methods yields three ordered components of the averaged P wave for each 5-min window analyzed.

Three P-wave morphology features are computed to characterize those averaged P waves: the power of the i-th transformed component, $\mathcal{P}_i^{\Psi}$, $i \in \{1, 2, 3\}$, $\Psi \in \{\text{PCA}, \pi\text{CA}\}$, the relative power of the second-to-first component, $\mathcal{P}_2^{\Psi,r} = \mathcal{P}_2^{\Psi}/\mathcal{P}_1^{\Psi}$, the relative power of the third to the first plus the second component, $\mathcal{P}_3^{\Psi,r} = \mathcal{P}_3^{\Psi}/(\mathcal{P}_1^{\Psi} + \mathcal{P}_2^{\Psi})$ and a measure of rugosity is taken as the power of the P wave after high-pass filtering with a 30 Hz cut-off frequency, $\mathcal{P}_1^{\Psi,\text{HF}}$.

In addition, the P-wave duration is measured using the delineator in [7] on the first transformed lead (PCA or πCA). We measure the mean duration of the P waves on the first principal and first periodic component, D_m^{Ψ}, within the 5-minute signal excerpts.

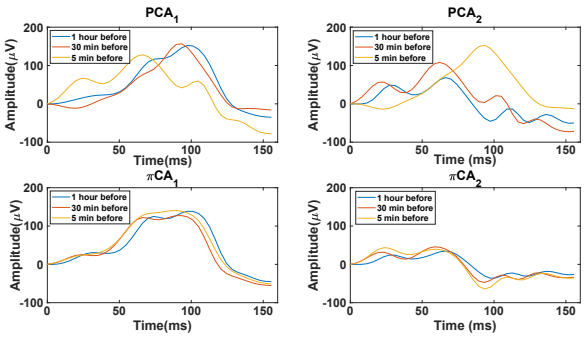

Figure 3. Temporal evolution, in the minutes previous to the first PxAF event in recording #13, of the averaged P wave at the a)first PCA lead b)second PCA lead c)first πCA lead and d) second πCA lead

3.5. Statistical analysis

We consider the records of different subjects as observations of the same phenomenon. A non-parametric method, *Wilcoxon signed rank test*, was used to compare the features at the different times previous to an AF episode. The null hypothesis was rejected when $p \leq 0.05$ for pairwise comparisons and $p \leq 0.05/\alpha$, with $\alpha = 3$, for comparisons between the three excerpts, accounting for *Bonferroni* correction.

4. Results

Figure 3 shows the temporal evolution of the transformed P wave using PCA and πCA, respectively, during the minutes previous to the first valid AF episode in recording #13. Specifically, they show the temporal evolution of average P wave on the first and second PCA (3a y b) and first and second πCA transformed leads (3c y d). Table 1 shows median and interquartile range (IQR) of all the features described in section 3.4.

The power of the first three transformed leads using PCA and using πCA did not present significant differences along the time.

On the other hand, significant changes were observed in the relative power of second-to-first principal component, $\mathcal{P}_2^{\text{PCA,r}}$, but were not found in the relative power of the second-to-first periodic component, $\mathcal{P}_2^{\pi\text{PCA,r}}$. Actually a significant increase was found from 60 to 30 min in the relative power of the second-to-first principal component ($p = 0.009$), and also from 60 to 5 min ($p = 0.002$).

Neither the relative power of the third to the first plus the second component and high-frequency powers showed significant differences along the time using both methods.

Regarding to the P-wave duration of the first principal component, D_m^{PCA}, and P-wave duration of the first peri-

odic component, $D_m^{\pi CA}$, both of them showed significant differences as AF approached. The mean duration of the first principal component of the P wave, showed a significant increase from 60 to 5 min (from 112.8 to 116.8 ms, $p = 0.005$), and also the mean duration of the first periodic component, significantly increased from 60 to 5 min (from 105.1 to 109.0 ms, with $p = 0.011$).

Table 1. Features, evolution at the selected time instants previous to PxAF events, Median[IQR]. Boldface types indicate significant differences versus 60 min with p<0.016

		60 min	**30 min**	**5 min**
PCA	$\mathcal{P}_1^{PCA}$	309.3[423.6]	330.7[369.7]	297.7[419.6]
	$\mathcal{P}_2^{PCA}$	46.2[65.4]	48.1[62.1]	49.9[70.4]
	$\mathcal{P}_3^{PCA}$	4.1[13.7]	4.3[11.6]	4.6[12.9]
	$\mathcal{P}_2^{PCA,r}$	0.127[0.164]	**0.139[0.172]**	**0.150[0.257]**
	$\mathcal{P}_3^{PCA,r}$	0.014[0.030]	0.013[0.021]	0.014[0.035]
	$\mathcal{P}_1^{PCA,HF}$	0.56[0.63]	0.57[0.57]	0.52[0.54]
	D_m^{PCA}	112.8[23.3]	116.0[23.3]	**116.8[23.2]**
πCA	$\mathcal{P}_1^{\pi CA}$	140.4[257.6]	128.0[262.1]	139.8[252.2]
	$\mathcal{P}_2^{\pi CA}$	29.6[59.4]	31.6[58.0]	35.1[60.2]
	$\mathcal{P}_3^{\pi CA}$	2.3[4.4]	1.9[5.2]	2.3[5.1]
	$\mathcal{P}_2^{\pi CA,r}$	0.162[0.294]	0.188[0.374]	0.191[0.320]
	$\mathcal{P}_3^{\pi CA,r}$	0.012[0.021]	0.013[0.019]	0.013[0.023]
	$\mathcal{P}_1^{\pi CA,HF}$	0.21[0.37]	0.21[0.35]	0.18[0.38]
	$D_m^{\pi CA}$	105.1[31.1]	108.0[31.1]	**109.0[31.1]**

5. Discussion

In patients with PxAF, despite $\mathcal{P}_2^{PCA}$ did not show any significant differences along time, $\mathcal{P}_2^{PCA,r}$ increased as AF episodes approached. This can be interpreted as an increase the complexity of the P-wave loop as the AF episodes approached.

The $\mathcal{P}_2^{\pi CA}$ and the $\mathcal{P}_2^{\pi CA,r}$ did not show any significant differences. Therefore, we cannot assert that there is a change in the repeatibility of the wavefront. No significant differences were found in the high frequency power, $\mathcal{P}_1^{\Psi,HF}$, with any of the methods.

Mean P-wave duration of the first principal and periodic component increased from 60 min to 5 min. This P-wave widening could be an effect of slowing down the conduction velocity or a more complex propagation throughout the atria when AF episodes approaches.

The results here obtained should be further investigated in larger populations to confirm or not the clinical markers significance as predictors to AF episodes. While this work focused in the changes of the averaged P wave within the 60 min previous to AF episodes, the study of the dynamics of the P wave in the few minutes immediately preceding AF episodes could show more clear changes.

6. Conclusions

The study shows that P-wave morphology significantly change prior to the onset of AF episodes leading to a more complex P-wave loop and enlarging the duration, which can be attributed to the de-structuring of atrial wavefront.

Acknowledgments

This work was supported by the Science and Innovation Spanish Ministry: PID2019-105674RB-I00 and PID2019-104881RB-I00 and by Gobierno de Aragon (Reference BSICoS: T39-20R) co-funded by FEDER 2014-2020.

References

[1] Fuster V, Rydén LE, Cannom DS, Crijns HJ, Curtis AB, Heuzey JYL. ACC/AHA/ESC 2006 Guidelines for the management of patients with atrial fibrillation. J Am Coll Aug. 2006;8(9):651–745.

[2] Laslett L, Jr PA, 3rd BC, Jr JD, Saldivar F, Wilson S, Poe C, Hart M. The worldwide environment of cardiovascular disease. J Am Coll Dec. 2012;60(25):S1–49.

[3] Platonov P. P-wave morphology: Underlying mechanisms and clinical implications. ANE Jul. 2012;17(3):161–169.

[4] Censi F, Corazza I, Reggiania E, Calcagnini G, Mattei E, M MT, Boriani G. P-wave variability and atrial fibrillation. Sci Rep May. 2016;6(26799).

[5] Henriksson M, Martín-Yebra A, Butkuvienė M, Rasmussen JG, Marozas V, Petrėnas A, Savelev A, Platonov PG, Sörnmo L. Modeling and estimation of temporal episode patterns in paroxysmal atrial fibrillation. IEEE Trans Biomed Eng 2021;68(1):319–329.

[6] Laguna P, Sörnmo L. Bioelectrical signal processing in cardiac and neurological applications. Burlington 2005;.

[7] Martinez J, R.Almeida, Olmos S, Rocha A, Laguna P. A wavelet-based ecg delineator:evaluation on standard db. IEEE TransBiomedEng Sep. 2004;51(4):570–581.

[8] Petrènas A, Sörnmo L, Lukosevicius A, Marozas V. Detection of occult paroxysmal atrial fibrillation. Med Biol Eng Comput Apr. 2015;53(4):287–297.

[9] Monasterio V, Clifford G, Laguna P, Martínez J. A multilead scheme based on periodic component analysis for t-wave alternans analysis in the ecg. Ann Biomed Eng Aug. 2010;38(8):2532–2541.

[10] Sameni R, Jutten C, Shamsollahi M. Multichannel electrocardiogram decomposition using periodic component analysis. IEEE Trans Biomed Eng Aug. 2008;55(8):1935–1940.

[11] Saul L, Allen J. Periodic component analysis: An eigenvalue method for representing periodic structure in speech. Advances in Neural Information Pro Jan. 2000;807–813.

Address for correspondence:

Cristina Moreno

Campus Río Ebro. Mariano Esquillor,S/N.50018 Zaragoza,Spain

cmorenoa@unizar.es